ADVANCED MATERIALS
www.advmat.de

In Situ Tracking of Wetting-Front Transient Heat Release on a Surface-Mounted Metal–Organic Framework

Weijin Li, Guang Yang, Alexandros Terzis, Soumya Mukherjee, Chao He, Xingtao An, Jingyi Wu, Bernhard Weigand, and Roland A. Fischer**

Transient heat generation during guest adsorption and host–guest interactions is a natural phenomenon in metal–organic framework (MOF) chemistry. However, in situ tracking of such MOF released heat is an insufficiently researched field due to the fast heat dissipation to the surroundings. Herein, a facile capillary-driven liquid-imbibition approach is developed for in situ tracking of transient heat release at the wetting front of surface-mounted MOFs (SURMOFs) on cellulosic fiber substrates. Spatiotemporal temperature distributions are obtained with infrared thermal imaging for a range of MOF-based substrates and imbibed liquids. Temperature rises at the wetting front of water and binary mixtures with organic solvents are found to be over 10 K with an ultrafast and distinguishable thermal signal response (<1 s) with a detectable concentration limit ≤1 wt%. As an advancement to the state-of-the-art in trace-solvent detection technologies, this study shows great prospects for the integration of SURMOFs in future sensor devices. Inspired by this prototypal study, SURMOF-based transient heat signal transduction is likely to be extended to an ever-expanding library of SURMOFs and other classes of surface-grafted porous materials, translating into a wide range of convenient, portable, and ubiquitous sensor devices.

Metal–organic frameworks (MOFs) are a class of crystalline materials with tailorable porosity, structural diversity and chemical tunability wherein specific gas or liquid species can be adsorbed, stored and released for further use.[1–3] In principle, many MOFs can release heat during adsorption including chemisorption and physisorption where the latter is largely driven by host–guest interactions such as H-bonds formation and van der Waals forces, among others.[4–7] It is a standard research practice to study such transient heat releases in order to understand the adsorption thermodynamics and kinetics behavior of MOFs, contextualizing varying degrees of interactions with the adsorbates.[8–10] However, exploring MOF transient heat in practical applications such as in corresponding sensor devices, is an uncharted territory due to the quick heat dissipation to the surroundings.

As a porous material, cellulosic fiber paper (CFP) is able to spontaneously transport water accompanied by a weak temporary temperature rise at the wetting front.[11,15] The capillary force induced by interfacial energy differences and electrostatic attractions that occur at the dry–wet crossover region are the key contributing factors.[11–14] Such capillary-driven spontaneous water imbibition studies indicate that the transient heat produced by adsorption and chemical interactions can be monitored by the simple use of thermometers. However, the temperature rise at the CFP wetting front is relatively small (<4 K) and non-selective in the context of translating into potential sensing devices.[10,14,15] This is largely because of two factors: weak water adsorption capacity and the lack of modularity in

Dr. W. J. Li, Dr. S. Mukherjee, Prof. R. A. Fischer
Chair of Inorganic and Metal-Organic Chemistry
Catalysis Research Center
Ernst-Otto-Fischer Straße 1 and Department of Chemistry
Technical University of Munich
Lichtenbergstraße 4, Garching bei München 85748, Germany
E-mail: roland.fischer@tum.de

The ORCID identification number(s) for the author(s) of this article can be found under https://doi.org/10.1002/adma.202006980.

[+]Present address: Faculty of Aerospace Engineering, Technion-Israel Institute of Technology, Haifa 3200003, Israel

Dr. G. Yang, Prof. J. Y. Wu
School of Mechanical Engineering
Shanghai Jiao Tong University
Dongchuan Road 800, Shanghai 200240, China
E-mail: y_g@sjtu.edu.cn

Dr. A. Terzis[+]
Department of Mechanical Engineering
Stanford University
Stanford, CA 94305, USA

Dr. C. He, Prof. X. T. An
School of Sciences
Hebei University of Science and Technology
Yuxiang Street 26, Shijiazhuang 050018, China

Prof. B. Weigand
Institute of Aerospace Thermodynamics
University of Stuttgart
Pfaffenwaldring 31, Stuttgart 70569, Germany

DOI: 10.1002/adma.202006980

the CFP architecture.[15,16] Hydrophilic porous MOFs with tailored architecture could potentially show a high water adsorption capacity based on either chemisorption and physisorption, each process inflicting a temperature increase when fabricating them as thin films.[17] To date, some MOFs have been deposited on filter and cellulose fiber paper substrates by different methods (e.g., dip-coating, vacuum filtration, and solvothermal methods) to serve the applications of gas adsorption and separation, and antibacterial tests (Table S1, Supporting Information). Among these MOFs, one of the most widely studied and cost-efficient MOFs until now, copper 1,3,5-benzenetricarboxylate, $[Cu_3(BTC)_2]$[18] widely known as HKUST-1 features hydrophilic properties and due to its microporous channels and coordinatively unsaturated Cu(II) centers, demonstrates high water uptake in ambient environment.[19] In synergy with the facile thin film fabricating approach, HKUST-1 could be a promising example for the initial trials in exploring MOF transient heat relevant to a range of potential applications.

In this work, inspired by the natural phenomenon of transient heat produced by host–guest interactions, we demonstrate that HKUST-1 can be fabricated on CFP surface through layer-by-layer method. This enables us, herein, to track the transient heat in situ, culminating in a trace liquid sensor model (Video S1, Supporting Information). This surface-mounted MOF (SURMOF) prototype synergistically enables strengthening and visualizing the transient heat generated from spontaneous imbibition of water in the form of a versatile signal transduction, particularly relevant to sensing applications.[20–23] HKUST-1 is built from hydrophilic Cu(II) sites that facilitate strong water affinity (**Figure 1**a–c). The energy released from its water adsorption, ≈50 kJ mol^{-1} is much larger than its transient heat[24] of hydrogen bonding formation ≈3 kJ mol^{-1}, which could result in a temperature rise of >10 K at the wetting front.

According to the Young–Laplace equation (Equation S1, Supporting Information), the capillary pressure that drives the liquid motion is inversely proportional to the effective pore radius while being proportional to the cosine of the contact angle formed in the solid–liquid interface.[25] The interconnected microporous channels in HKUST-1 are, therefore, likely to elicit strong capillary actions during spontaneous imbibition of water. Besides, HKUST-1 being replete with open Cu(II) sites (Figure 1b,c) further augments water uptake. Therefore, surface-mounted HKUST-1 (SURHKUST-1) for ultrafast (<1 s) and highly sensitive (<1 wt%) response to a single trace solvent such as water from its mixtures with other solvents exemplifies an unexplored area of high potential. To the best of our knowledge, this study is the first report of quantifying transient heat released at the microfluidic SURMOF wetting front. Upon improvement, the presented results can be potentially harnessed in improving signal transductions. This targets remediation of trace contamination by solvent sensing including trace water quantification (Table S2, Supporting Information). Introduction of such an inclusive approach should lead to

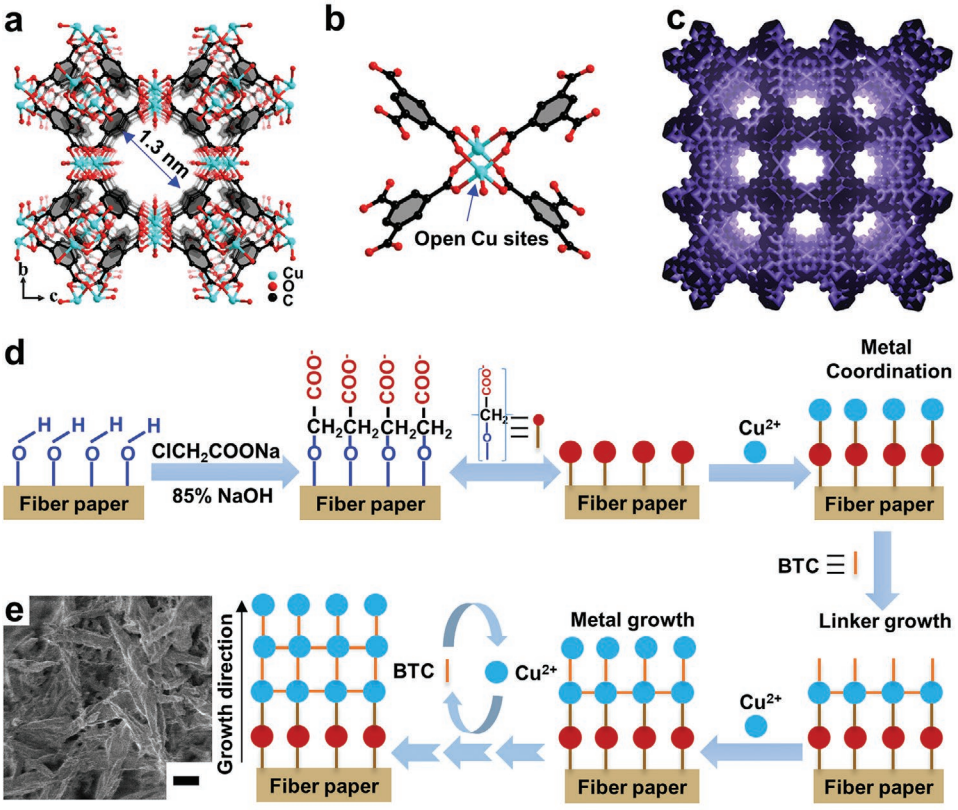

Figure 1. a) Crystal structure of HKUST-1: viewed along crystallographic *a*-axis including the 1D channel dimension. b) A single Cu(II) paddle wheel secondary building unit constituting HKUST-1, comprising two open Cu(II) sites. c) Connolly surfaces (marked in violet) affording interconnected cavities. d) Preparation of SURHKUST-1 on CFP. e) SEM image of SURHKUST-1 (60 cycles); scale bar: 1 µm.

a widespread integration of MOFs on flexible and low-cost paper substrate, affording cheap and portable thin film devices (Table S3, Supporting Information) for liquid content determination, e.g., water, methanol, and ethanol from fuel oil, liquor, and alcoholic beverages.[26–28] In essence, this portable method enables easier operation and faster detection versus currently reported Karl Fischer titration, chromatography, and other MOF sensors based signal transduction (Table S4, Supporting Information).

Preparation of SURHKUST-1 on CFP is depicted in Figure 1d. SURHKUST-1 was deposited as self-assembled monolayers (SAMs) on CFPs through layer-by-layer (LBL) approach[29] by first immersing the pre-treated CFP in a solution of Cu(II), then subjected to ethanol wash and finally immersed in H_3BTC solution, with repetition of the whole cycle (Figure S1, Supporting Information). The grazing-incidence X-ray diffraction (GIXRD) pattern was indicative of phase purity for the deposited HKUST-1 on CFP (Figure S2, Supporting Information). Attenuated total reflection infrared (ATR-IR) spectra of the SURHKUST-1 agreed with those of the bulk HKUST-1, confirming the composition of HKUST-1 on CFP (Figure S3, Supporting Information). Scanning electron microscopy (SEM) images indicate that HKUST-1 was uniformly mounted on CFP surface (Figure 1e; Figure S4, Supporting Information). The needle-like grain size of HKUST-1 crystallites was found to increase with increasing deposition cycles, ranging from ≈20 to ≈500 nm, a factor likely to be associated with sensing responses.[30–32] This evidence confirms that well-controlled SURHKUST-1 could be obtained on CFPs via the LBL method.

The amphipathic character of the SURMOFs is a key feature to induce adsorption-based sensing applications.[33,34] Water, methanol and *n*-hexane isotherms of SURHKUST-1 were recorded; all conformed to typical type-I nature with the highest saturation uptake registered for water, suggesting a hydrophilic microporosity in SURHKUST-1 (Figure S5, Supporting Information).[32] Furthermore, static water contact angle of SURHKUST-1 was measured to be 0° (Figure S6, Supporting Information) and dynamic water contact angle measurement shows that water droplet rapidly penetrated into the MOF thin film layer upon falling off (Video S2, Supporting Information). This evidence reinforces the high hydrophilicity

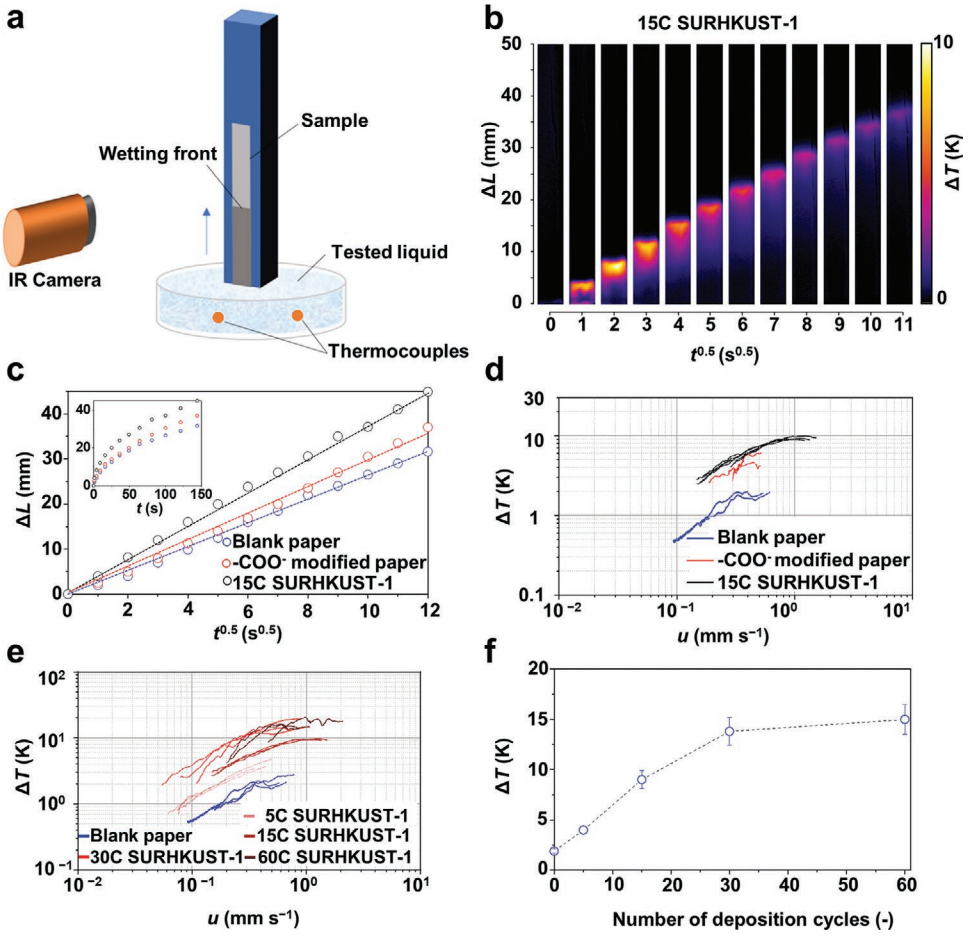

Figure 2. a) Setup for measuring the temperature rise. b) Thermal images of 15 deposition cycles of SURHKUST-1 (denoted as 15C SURHKUST-1) capillary filling with water. c) Capillary dynamics of water in papers obtained from different treatments. Here, $t = 0$ defines the moment that the CFPs contact water. d,e) Level of temperature rise as a function of imbibition speed to ensure complete wetting of the papers: d) effect of different treatments and e) effect of HKUST-1 deposition cycles. f) Local temperature rise at the wetting front as a function of the number of HKUST-1 deposition cycles, measured 10 mm away from the bottom of the SURHKUST-1 sample.

(considering both pore and surface) of the SURHKUST-1 thin films.[32]

Drawing advantages from the capillary-driven spontaneous imbibition and the superhydrophilicity of HKUST-1,[35,36] the transient heat release can be continuously monitored by using in situ temperature sensing tools, such as thermocouples, resistance temperature detectors (RTDs), and infrared cameras (**Figure 2**a; Table S3, Supporting Information). As anticipated, temperature rises in SURHKUST-1 is found significantly larger than that observed in blank CFP (Figure 2b; Figure S7, Supporting Information). This is attributed to the hydrophilic properties of SURHKUST-1 possessing a high-water adsorption ability, as well as the heat release accompanying adsorption.[37] The capillary-driven imbibition height (ΔL) is found to hold a linear relationship with $t^{0.5}$, demonstrating a Washburn-like imbibition process (Figure 2c; Equations S2 and S3, Supporting Information).[38] This indeed validates the Washburn law in nanoporous materials exemplified by HKUST-1.[39] Steeper slopes of the lines suggest a faster capillary imbibition speed, one of the contributing factors to advance the function-driven applications related to response time. Despite manifesting an identical temperature rise, SURHKUST-1 exhibited a faster imbibition speed compared to the uncoated CFPs (Figure 2d,e). Interestingly, the temperature rise and imbibition speed can be expedited by simply increasing the deposition cycles during SURMOF fabrication (Figure 2f). To probe the intrinsic transient heat under capillary-driven water spontaneous imbibition, bulk powder of HKUST-1 was formulated into a pressed pellet and subjected to temperature rise (Figure S8, Supporting Information). The free-standing MOF tablet could be seen to exhibit a large temperature rise at the wetting front (Figure S9a, Supporting Information). This evidence suggests that HKUST-1 coated onto a CFP surface can intrinsically improve the microfluidic dynamic behavior and augments transient heat release at the wetting front of CFPs, thanks to a unison of long-range ordered porosity and hydrophilicity. Significantly, success of this approach refers to the scopes of extending it to several other MOFs, such as MIL-101 (Cr), MOF-801, and UiO-66 (Figure S9b, Supporting Information) in a task-specific manner. Recycling of adsorbent is critical to its practical use.[40] We also measured temperature rise at the wetting front of SURHKUST-1 for testing its feasibility to be recycled (Figures S10–S13, Supporting Information), an aspect considerably significant than that of an equivalent blank paper.

We envisage that different guest species are likely to show distinct energy changes upon getting adsorbed in MOFs and will result in significant temperature rises accompanying the solvent wetting fronts imbibing spontaneously, leaving fingerprints that enable their selective detection from mixtures. As a proof-of-concept, during capillary filling with different organic solvents, the temperature rise of the wetting front was measured (Figure S14a, Supporting Information). Each solvent also exhibits a distinct imbibition speed during wetting (Figure S14b, Supporting Information). The largely different temperature rises and discriminatory imbibition speeds offer the feasibility for utilizing SURHKUST-1 to detect trace water in organic solvents.

Considering water–ethanol and water–methanol solutions of varying volumetric compositions as typical examples, SURHKUST-1 was used to analyze water contents in these solutions. Between two distinct binary mixtures, SURHKUST-1 showed different temperature rises and imbibition speeds at the wetting front (**Figure 3**). Though the difference is tiny, below 1 wt%, the monotonous trend indicates that the detectable concentration of water is expected to further decrease with an increase of resolutions of the temperature sensors in future

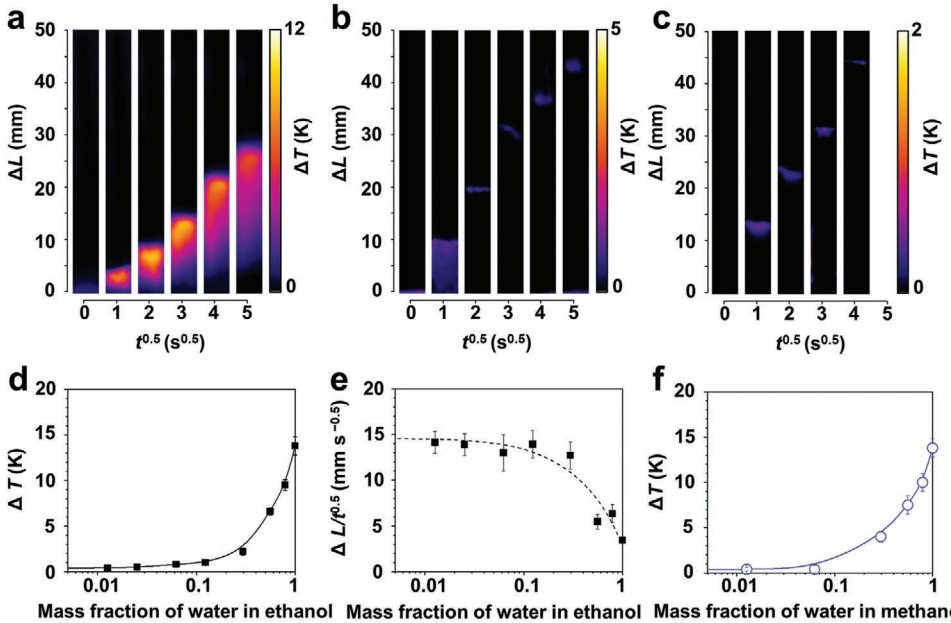

Figure 3. a–c) Thermal images of capillary filling with different ratios of ethanol/water (w/w): a) 20 wt% ethanol in water; b) 70 wt% ethanol in water; c) 93 wt% ethanol in water. d) Local temperature rises and e) imbibition speed, as a function of the fraction of water in ethanol, measured 10 mm away from the bottom of the SURHKUST-1 sample. f) Local temperature rises as a function of the mass fraction of water in methanol, measured 10 mm away from the bottom of the SURHKUST-1 sample.

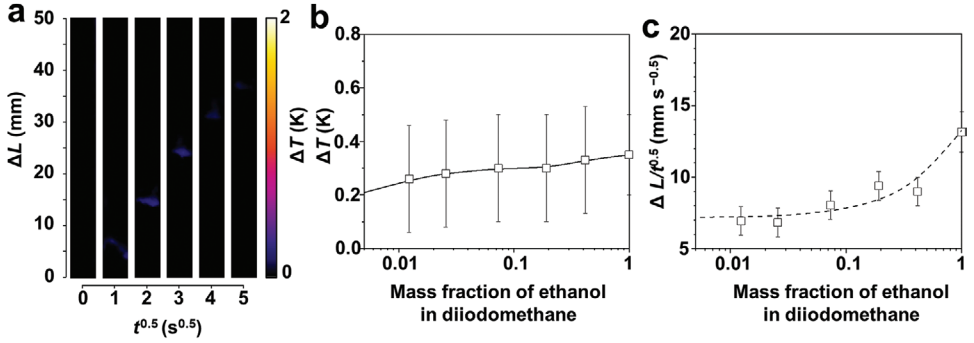

Figure 4. a) Thermal images of capillary imbibition at the wetting front of 30C SURHKUST-1 with [42 wt% ethanol/58 wt% diiodomethane] mixture. b) Local temperature rises as a function of the fraction of ethanol in diiodomethane, measured 10 mm away from the bottom of the SURHKUST-1 sample. c) Capillary imbibition speed as a function of the fraction of ethanol in diiodomethane. Error bars correspond to the uncertainty of four individual experiments.

(Figure 3d). The imbibition speeds for various concentrations are plotted in the form of (ΔL–$t^{-0.5}$), taking into account the Washburn-like imbibition behavior (Figure 3e; Equations S2 and S3, Supporting Information), which results in a steadily decreasing trend with an increase of the mass fraction of water at >10 wt%. Regarding trace water detection from methanol (Figure 3f), the variation of temperature rise with water concentration shows a similar trend to that observed in water–ethanol mixtures.

Notably, we can expand the currently discussed concept to distinguish transient heats originated from binary polar and nonpolar organic mixtures (**Figure 4**a). Both the temperature rises and the imbibition speeds increased with escalating mass fractions of ethanol in the ethanol–diiodomethane mixtures (Figure 4b,c). In principle, the working principle upholds to track the transient heat released by imbibition for ternary, quaternary, and more complex multicomponent liquid mixtures.[41–43] However, simplifying current studies of the "prototype," the complexities of multiple host–guest interactions and low camera resolution used here limits the scopes of the current experimental setup to ternary mixtures.

The heat release of wetting process shows a declining profile of heat content (i.e., enthalpy, $-\Delta H$) of SURMOF and liquid in the SURMOF–liquid system. Such variations in the decreasing enthalpy with temperature is ascribed to the different heat capacities between SURMOF and the respective solvent, before and after liquid wetting according to the Kirchhoff's equation (Equation S4, Supporting Information).[44]

As regards the CFP substrate, the dry CFP surface can adsorb liquid molecules due to the surface-exposed hydroxyl groups that form molecular interactions in terms of causing a heat release at the CFP–liquid interface.[45] However, the heat release phenomenon is often inconspicuous and only limited to liquids composed of polar molecules. MOFs, on the contrary, that feature tunable porous architecture, high surface area, and low density enable them with a high heat capacity. Based on the nature of guest-accessible voids, MOFs demonstrate entirely different adsorption behaviors while capturing the same guest molecule. Generally, the guest molecules adsorbed by MOFs interact with the MOF channels in one or both (cooperative mechanisms) of the following ways: i) energy-intensive chemisorption, involving direct bond formation and cleavage such as coordination to open metal sites, amine-grafting leading to CO_2 fixation, etc.; ii) energy-efficient physisorption that revolves around weaker bonds such as H-bonding, van der Waals forces etc.[46,47] As the CFP is chosen, the released transient heat responding to different guest molecules is mainly determined by the enthalpy change between MOFs and guest molecules. By exercising a rational choice on the composition of host MOF and to fabricate a SURMOF thereof, a specific heat release transduction signal raised by enthalpy change of the SURMOF toward different guest molecules can be utilized in recognizing solvents with specificity. To quickly estimate the enthalpy change of MOFs responding to different guest molecules, simple computational models based on a primitive cell of MOF adsorbing one guest molecule inside the pore and on surface were built (**Figure 5**). As shown in Figures S15 and S16 in the Supporting Information, HKUST-1 demonstrates different enthalpy changes toward the adsorption of one water, methanol, ethanol, *N*,*N*-dimethylformamide, acetonitrile, and acetone molecule. The studies reveal that HKUST-1 exhibits different temperature rises toward different solvents. In other representative MOFs such as MOF-801 and UiO-66, signature temperature rises in response to different guest molecules (Figures S17 and S18, Supporting Information) could be noted as well.

However, the released transient heat dissipates quickly upon direct immersion of SURMOF in the solvent. Spontaneous heat release at the wetting front could be visually monitored by a thermal camera with a descriptor of temperature rise. The capillary-action-driven spontaneous rise of the liquids through the porous structures is determined by measuring surface and interfacial tensions of the liquid and liquid–vapor interface respectively, each deduced by the Young–Laplace equation (Equations S1–S3, Supporting Information).[25]

These describe the key role of modularity in porous MOFs and how tunability in SURMOFs morphology can be leveraged to enable spontaneous imbibition of liquids in them. That the pore size, particle packing mode/alignment on the surface directly influence the process implies its reliance upon the spontaneous imbibition response speed.

We present a convenient, versatile, and scalable approach to in situ tracking of transient heat release during spontaneous imbibition of water and binary mixtures at the front surface of SURMOFs on CFP. The results demonstrate that the developed approach can be used as a fast method toward selectively detecting trace liquid residues from a variety of organic solvents. The selectivity and sensitivity of SURMOFs

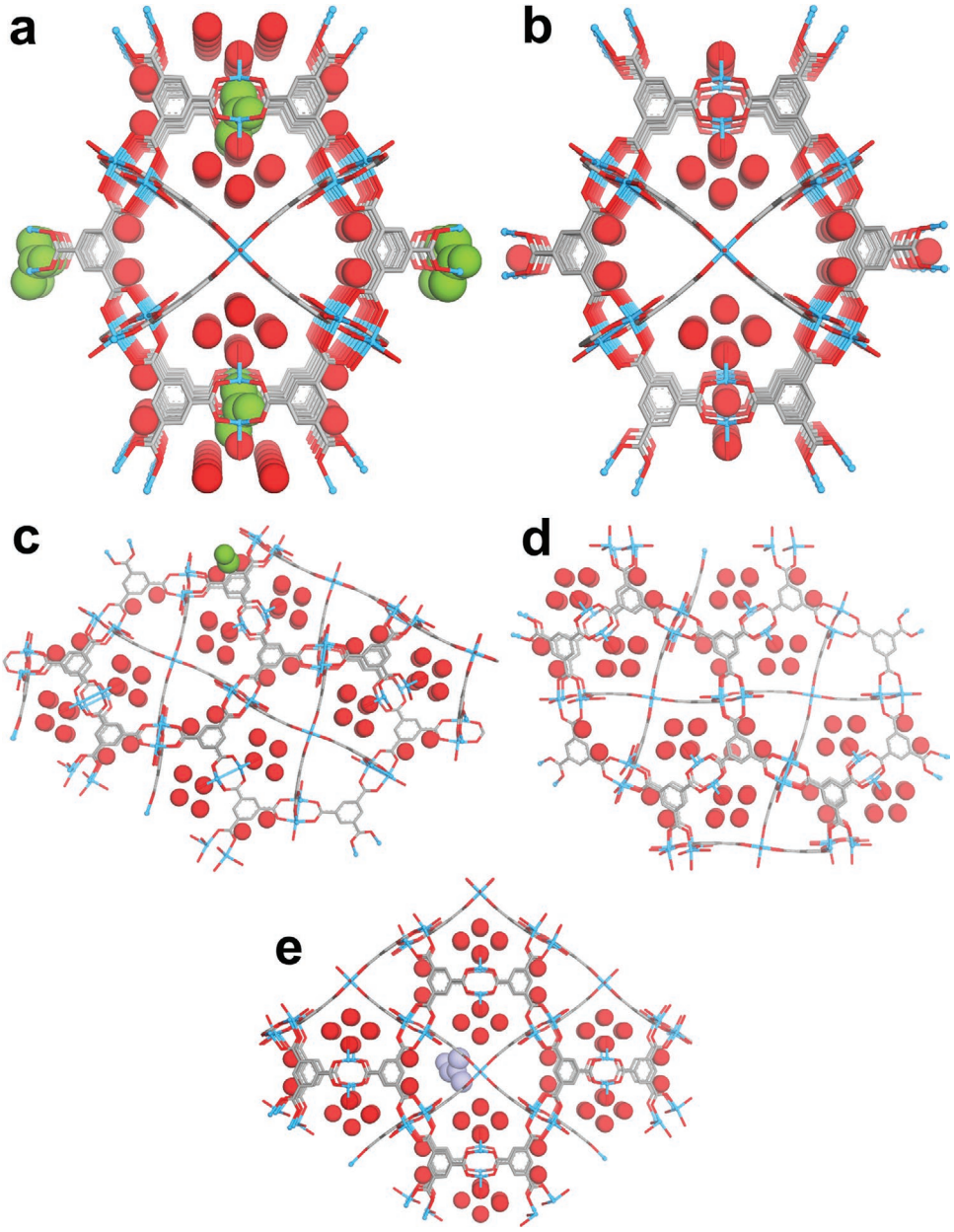

Figure 5. a–e) Simulated models of the guest-adsorbed phases: a,b) adsorption inside the pore for guest molecules acetone and water, respectively; c–e) surface adsorption for methanol, water, and DMF respectively. Color codes: grey: carbon, blue: copper, red: oxygen. For (a,b) the olive green spheres shown in space-filling model refer to guest acetone molecules whereas the red spheres shown in space-filling model denote guest water molecules. For (c–e) the olive green, red and lilac spheres shown in space-filling model refer to the surface-adsorbed guests: acetone, water, and *N*,*N*-dimethylformamide molecules respectively.

response to trace residues is found amenable to systematic fine-tuning of the deposition cycles and engineering of the controlled deposition techniques. We consider this counterintuitive approach, which requires simple instrumentation, to be likely of general relevance thanks to the steadily growing library of easy-to-synthesize SURMOFs. Building upon this reported prototype, we envision that the method of treating capillary-driven spontaneous wetting front heat release as a signal transduction metric will afford several examples relevant to the ambitious development of ergonomic sensor devices.

Supporting Information

Supporting Information is available from the Wiley Online Library or from the author.

Acknowledgements

W.L. and G.Y. contributed equally to this work. W.L. and S.M. gratefully acknowledge the Alexander von Humboldt Foundation for their postdoctoral research fellowships. G.Y. kindly acknowledges the support of the National Natural Science Foundation of China

(Grant No. 51906142) and Shanghai Pujiang Program (Grant No. 19PJ1405600). The authors appreciate Prof. Tianfu Liu (Fujian institute of research on the structure of matter, Chinese Academy of Sciences) for providing with MOFs powders of MIL-101(Cr), MOF-801 and UiO-66, Dr. Juan Liu (Department of Chemistry, Technical University of Munich, Germany) for the discussion of the manuscript, and Dr. Huiyan Zhao from Department of Physics and Hebei Advanced Thin Film Laboratory, Hebei Normal University for the help regarding theoretical calculations.

Open access funding enabled and organized by Projekt DEAL.

Conflict of Interest

The authors declare no conflict of interest.

Data Availability Statement

The data that support the findings of this study are available from the corresponding author upon reasonable request.

Keywords

host–guest adsorption, liquid imbibition, metal–organic framework thin films, sensor devices, transient heat

Received: October 13, 2020
Revised: December 17, 2020
Published online: February 24, 2021

[1] J. D. Evans, B. Garai, H. Reinsch, W. J. Li, S. Dissegna, V. Bon, I. Senkovska, R. A. Fischer, S. Kaskel, C. Janiak, N. Stock, D. Volkmer, *Coord. Chem. Rev.* **2019**, *380*, 378.
[2] J. Y. Lee, O. K. Farha, J. Roberts, K. A. Scheidt, S. T. Nguyen, J. T. Hupp, *Chem. Soc. Rev.* **2009**, *38*, 1450.
[3] W. Schrimpf, J. C. Jiang, Z. Ji, P. Hirschle, D. C. Lamb, O. M. Yaghi, S. Wuttke, *Nat. Commun.* **2018**, *9*, 1647.
[4] C. Schlüsener, M. Xhinovci, S.-J. Ernst, A. Schmitz, N. Tannert, C. Janiak, *Chem. Mater.* **2019**, *31*, 4051.
[5] S. K. Henninger, H. A. Habib, C. Janiak, *J. Am. Chem. Soc.* **2009**, *131*, 2776.
[6] A. J. Rieth, A. M. Wright, S. Rao, H. Kim, A. D. LaPotin, E. N. Wang, M. Dincă, *J. Am. Chem. Soc.* **2018**, *131*, 17591.
[7] J. Wieme, S. Vandenbrande, A. Lamaire, V. Kapil, L. Vanduyfhuys, V. V. Speybroeck, *ACS Appl. Mater. Interfaces* **2019**, *11*, 38697.
[8] V. Bon, I. Senkovska, J. D. Evans, M. Wöllner, M. Hölzel, S. Kaskel, *J. Mater. Chem. A.* **2019**, *7*, 12681.
[9] Z. G. Hu, Y. X. Wang, B. B. Shah, D. Zhao, *Adv. Sustainable Syst.* **2019**, *3*, 1800080.
[10] H. Babaei, M. E. DeCoster, M. Jeong, Z. M. Hassan, T. Islamoglu, H. Baumgart, A. J. H. McGaughey, E. Redel, O. K. Farha, P. E. Hopkins, *Nat. Commun.* **2020**, *11*, 4010.
[11] J. W. Barnett, M. R. Sullivan, J. A. Long, D. Tang, T. Nguyen, D. Ben-Amotz, B. C. Gibb, H. S. Ashbaugh, *Nat. Chem.* **2020**, *12*, 589.
[12] H. Aslannejad, A. Terzis, S. M. Hassanizadeh, B. Weigand, *Sci. Rep.* **2017**, *7*, 7268.
[13] A. Terzis, G. Yang, I. Zarikos, E. Elizalde, B. Weigand, A. Kalfas, X. Ding, *Microfluid. Nanofluid.* **2018**, *22*, 35.
[14] A. Terzis, E. Roumeli, K. Weishaupt, S. Brack, H. Aslannejad, J. Groß, S. M. Hassanizadeh, R. Helmig, B. Weigand, *J. Colloid. Interface Sci.* **2017**, *504*, 751.
[15] Cellulose Fiber—Definition of cellulose fiber in the Free Online Dictionary. The Free Online Dictionary. Retrieved December 7, 2014.
[16] K. Stana-Kleinschek, V. Ribitsch, T. Kreze, L. Fras, *Mater. Res. Innovations* **2002**, *6*, 13.
[17] S. Cui, A. Marandi, G. Lebourleux, M. Thimon, M. Bourdon, C. Chen, M. I. Severino, V. Steggles, F. Nouar, C. Serre, *Appl. Therm. Eng.* **2019**, *161*, 114135.
[18] S. S.-Y. Chui, S. M.-F. Lo, J. P. H. Charmant, A. G. Orpen, I. D. Williams, *Science* **1999**, *283*, 1148.
[19] J. B. DeCoste, G. W. Peterson, B. J. Schindler, K. L. Killops, M. a. Browe, J. J. Mahle, *J. Mater. Chem. A* **2013**, *1*, 11922.
[20] M. Allendorf, R. H. Dong, X. L. Feng, S. Kaskel, V. Stavila, D. Matoga, *Chem. Rev.* **2020**, *120*, 8581.
[21] L. E. Kreno, K. Leong, O. K. Farha, M. Allendorf, R. P. Van Duyne, J. T. Hupp, *Chem. Rev.* **2012**, *112*, 105.
[22] L. Chen, J.-W. Ye, H.-P. Wang, M. Pan, S.-Y. Yin, Z.-W. Wei, L.-Y. Zhang, K. Wu, Y.-N. Fan, C.-Y. Su, *Nat. Commun.* **2017**, *8*, 15985.
[23] W. P. Lustig, S. Mukherjee, N. D. Rudd, A. V. Desai, J. Li, S. K. Ghosh, *Chem. Soc. Rev.* **2017**, *46*, 3242.
[24] M. K. Bhunia, J. T. Hughes, J. C. Fettinger, A. Navrotsky, *Langmuir* **2013**, *29*, 8140.
[25] P. G. De Gennes, *Rev. Mod. Phys.* **1985**, *57*, 827.
[26] MAN B&W Two-stroke engines, https://manualzz.com/doc/28268106/guidelines-for-fuels-and-lubes-purchasing-operation-on-heavy (accessed: February 2021).
[27] M. Tomassetti, R. Angeloni, M. Castrucci, E. Martini, L. Campanella, *Acta Imeko* **2018**, *7*, 91.
[28] M. Tomassetti, R. Angeloni, S. Marchiandi, M. Castrucci, M. P. Sammartino, L. Campanella, *Sensors* **2018**, *18*, 3596.
[29] W. Li, S. Watzele, H. A. El-Sayed, Y. C. Liang, G. Kieslich, A. S. Bandarenka, K. Rodewald, B. Rieger, R. A. Fischer, *J. Am. Chem. Soc.* **2019**, *141*, 5926.
[30] L. Pan, G. Liu, W. Shi, J. Shang, W. R. Leow, Y. Q. Liu, Y. Jiang, S. Z. Li, X. Chen, R.-W. Li, *Nat. Commun.* **2018**, *9*, 3813.
[31] C. R. Marshall, S. A. Staudhammer, C. K. Brozek, *Chem. Sci.* **2019**, *10*, 9396.
[32] Y. Z. Chen, B. C. Gu, T. Uchida, J. D. Liu, X. C. Liu, X. C. Liu, B. J. Ye, Q. Xu, H.-L. Jiang, *Nat. Commun.* **2019**, *10*, 3462.
[33] K. Jayaramulu, F. Geyer, A. Schneemann, Š. Kment, M. Otyepka, R. Zboril, D. Vollmer, R. A. Fischer, *Adv. Mater.* **2019**, *31*, 1900820.
[34] X. Fang, B. Y. Zong, S. Mao, *Nanomicro Lett.* **2018**, *10*, 64.
[35] P. Z. Moghadam, T. Islamoglu, S. Goswami, J. Exley, M. Fantham, C. F. Kaminski, R. Q. Snurr, O. K. Farha, D. Fairen-Jimenez, *Nat. Commun.* **2018**, *9*, 1378.
[36] D. Lenzen, J. Zhao, S.-J. Ernst, M. Wahiduzzaman, A. K. Inge, D. Fröhlich, H. Y. Xu, H. J. Bart, C. Janiak, S. Henninger, G. Maurin, X. D. Zou, N. Stock, *Nat. Commun.* **2019**, *10*, 3025.
[37] T. Tian, Z. Zeng, D. Vulpe, M. E. Casco, G. Divitini, P. A. Midgley, J. Silvestre-Albero, J. C. Tan, P. Z. Moghadam, D. Fairen-Jimenez, *Nat. Mater.* **2018**, *17*, 174.
[38] E. W. Washburn, *Phys. Rev.* **1921**, *17*, 273.
[39] D. I. Dimitrov, A. Milchev, K. Binder, *Phys. Rev. Lett.* **2007**, *99*, 054501.
[40] E. S. M. El-Sayed, D. Q. Yuan, *Green Chem.* **2020**, *22*, 4082.
[41] J. A. Gustafson, C. E. Wilmer, *Sens. Actuators, B* **2018**, *267*, 483.
[42] Z. Z. Xu, X. H. Xiong, J. B. Xiong, R. Krishna, L. B. Li, Y. L. Fan, F. Luo, B. L. Chen, *Nat. Commun.* **2020**, *11*, 3163.
[43] J. Oktawiec, H. Z. H. Jiang, J. G. Vitillo, D. A. Reed, L. E. Darago, B. A. Trump, V. Bernales, H. Li, K. A. Colwell, H. Furukawa, C. M. Brown, L. Gagliardi, J. R. Long, *Nat. Commun.* **2020**, *11*, 3087.
[44] G. Raj, *Thermochemistry, Advanced Physical Chemistry*, 35th ed., Goel Publishing House, Meerut, India **2009**, p. 232.
[45] C. Yamane, T. Aoyagi, M. Ago, K. Sato, K. Okajima, T. Takahashi, *Polym. J.* **2006**, *38*, 819.
[46] I. Ahmed, S. H. Jhung, *Chem. Eng. J.* **2017**, *310*, 197.
[47] J. R. Li, J. Sculley, H.-C. Zhou, *Chem. Rev.* **2012**, *112*, 869.